JOURNAL OF MATERIALS SCIENCE 29 (1994) 3791–3796

Oxidation of ultrafine (Si–)SiC powders

R. VABEN, D. STÖVER
Institut für Werkstoffe der Energietechnik, Forschungszentrum Jülich GmbH, D-52425 Jülich, Germany

The increasing usage of ultrafine ceramic powders in the fabrication of highly reliable ceramics results in a growing interest in appropriate processing conditions for these powders. During processing the extremely high surface areas might lead to significant absorbtion of oxygen even at low temperatures. But especially in this temperature regime, oxidation data of powders are rarely available; as far as the authors know, no investigations have been published in the case of ultrafine powders with particle sizes below 100 nm. In this study the oxidation kinetics of ultrafine (Si–) SiC powders ($\sim$ 20 nm) in the temperature range between room temperature and 1000 °C in air were investigated. Thermobalance experiments showed that at least three different oxidation mechanisms are operating. At temperature above 650 °C the fraction of completion R is proportional to the square root of time, indicating a diffusion-controlled mechanism (activation energy $\simeq 1.8$ eV). At lower temperatures the best data fit is obtained by a Cabrera–Mott-like equation. At room temperature and for thin silica-layer thicknesses a third oxidation mechanism was determined. The formation of the first monolayer of silicon oxide obeys the kinetics of a first-order reaction, namely an exponential one with a time constant of $1.25 \times 10^{-4}\ s^{-1}$. An investigation of the influence of oxygen pressure on the oxidation of ultrafine Si–SiC powders revealed a low pressure influence at 500 °C. An approximately linear relation between pressure and oxidation rate constant is observed between 30 and 1000 mbar air pressure at 800 °C. The kinetic data were used to construct an "oxidation map" for ultrafine SiC powders, as a help to determine appropriate processing conditions.

1. Introduction

Due to the formation of a silica layer, SiC powders and ceramics are thermally stable up to very high temperatures. Numerous studies have been carried out to analyse the high-temperature oxidation of bulk materials [1–3]. Considerable work has also been conducted to investigate the oxidation kinetics of SiC powders, most of the work being performed in the temperature region above 800 °C and using powders with grain sizes larger than 10 μm (several investigations are discussed in the Gmelin Handbook [4]). An extrapolation of these parabolic rate constants down to low temperatures and down to ultrafine particle sizes (20 nm) is erroneous due to large differences between the activation energies given by different authors. An extrapolation using a low activation energy (1.2 eV [3]) leads to a rate constant of about $10^{-8}\ nm^2\ year^{-1}$. This low value cannot explain our experimental observation that the oxygen content of ultrafine silicon carbide powders increases significantly if they are stored at room temperature in air for several months. A possible explanation might be a change in the oxidation mechanism at low temperatures. This is observed in silicon at about 500 °C [5]. Silicon also forms a silica layer during oxidation and therefore the oxidation kinetics are similar to those of SiC. On the other hand the usage of the large database available for silicon oxidation (e.g. [6]) is only helpful to compare with actual SiC data because large differences often exist between the rate constants in silicon and SiC [3].

The purpose of this study was to perform low-temperature oxidation experiments to extend the database of the SiC oxidation down to temperatures below 800 °C. Ultrafine powders are excellent candidates for these investigations because even extremely small changes in the silica layer thickness can be detected by a conventional thermobalance (the growth of one monolayer of silica on a 20 nm SiC particle results in a mass change of more than 1%).

2. Experimental procedure

The ultrafine (Si–)SiC powders used in this study were produced at the Institut für Laser- und Plasmaphysik, Universität Düsseldorf (Germany), by CO_2 laser-assisted synthesis using a mixture of SiH_4 and $C_2H_2(C_2H_4)$ as gas-phase precursors [7]. The particle size measured by a transmission electron microscope (TEM) was 20 ± 2 nm. Chemical analysis (Leco system) of the SiC and Si–SiC powders revealed oxygen contents of 2.6 and 5.4 wt % and carbon contents of 29.4 and 7.6 wt %, respectively. The pressure dependence of the oxidation was investigated with Si–SiC powders having 8.6 wt % C and 7.1% O contents.

Between 100 and 300 mg of these powders were introduced in a thermobalance made by Linseis GmbH, Germany. The temperature was raised with

a heating rate of 10 K min^{-1} up to temperatures between 400 and 1000 °C. In the following the samples were isothermally oxidized for at least 5 h. To investigate the formation of the first silica layer, a cold isostatically pressed sample (470 mg) was washed with 3% HF and then cleaned with distilled water and ethanol. After this procedure the sample was immediately introduced into the thermobalance and the weight gain at room temperature measured for 20 h. The sample was then handled under argon until a chemical analysis was performed (oxygen: 1.75 wt %, carbon: 29.7 wt %). The relative humidity in our laboratory was in the range between 40 and 50% and the temperature was about 23 °C.

The oxygen content of ultrafine SiC powders stored in air for several months was also determined by chemical analysis. In this case the time interval between production and chemical analysis was taken as the effective oxidation period and the results were included in this study.

3. Results and discussion

3.1. Diffusion-controlled oxidation

The isothermal oxidation of powders is often described in terms of the well-known Jander equation [8]:

$$[1-(1-R)^{1/3}]^2 = \frac{2kt}{r^2} \quad (1)$$

where R is the fraction of the initial material which has reacted after the time t, k is the rate constant and r the initial particle radius. As pointed out by Carter [9] and Motzfeld [10], this equation is based on the assumption of equal molar volumes of the reaction product (SiO_2: ~ 27.3 cm^3) and the starting material (SiC: 12.5 cm^3) and is therefore valid only for $R \ll 1$. A more precise calculation [9, 10] leads to the equation.

$$f(R) = \frac{z^2}{z-1} - z(1-R)^{2/3} - \frac{z}{z-1}[1+(z-1)R]^{2/3} = \frac{2kt}{r^2} \quad (2)$$

where $z \simeq 2.18$ is the ratio between the molar volumes of the reaction product and the starting material. For $R < 0.4$ this equation can be approximated by a simple parabolic law with an error of less than 1% [10]:

$$R^2 = \frac{9}{z^2} f(R) = \frac{18kt}{z^2 r^2} \qquad R \ll 1 \quad (3)$$

For $R \to 1$ the function $f(R)$ approaches the final value 0.423.

The fraction of completion R can be calculated using the molar masses m_i of the participating species, the oxygen content determined in the chemical analysis, and the mass change $\Delta m/m$ measured by the thermobalance:

$$R = 2.038\frac{\Delta m}{m} + 0.0332 \qquad \text{SiC powder}$$

$$R = 1.26\frac{\Delta m}{m} + 0.0552$$

Si–SiC powder (1 bar, 400 and 500 °C) (4)

$$R = 1.32\frac{\Delta m}{m} + 0.0622$$

Si–SiC powder (pressure dependence)

The constants are added to take account of the oxidation before the actual thermobalance measurement.

In Fig. 1 the function $f(R)$ is plotted against time. The plateau at the end of the measurement at 1000 °C indicates a completion of the oxidation reaction. The final value (0.36) is about 16% below the theoretical one. Possible explanations are a slightly non-stoichiometric carbon concentration in the starting powder or the formation of gaseous SiO during the oxidation process. The zero point of time corresponds to the moment when the heating up of the samples starts. Least-square fits according to Equation 2 take account of this fact by subtracting a constant t_0 from the time t. For diffusion-controlled oxidation it is shown by the equation below that t_0 must be larger than zero and smaller than the time t_f, which is the time interval passing till the final oxidation temperature is reached:

$$f(R)*\frac{r^2}{2} = \int_0^t k(T)\mathrm{d}t = \int_0^{t_f} k[T(t)]\mathrm{d}t + \int_{t_f}^t k(T_f)\mathrm{d}t = \int_0^{t_f} k[T(t)]\mathrm{d}t + k_f(t-t_f) = k_f t^* + k_f(t-t_f) \quad (5)$$

with $0 \leqslant t^* \leqslant t_f$; here $0 \leqslant k \leqslant k_f \to 0 \leqslant t_0 = t_f - t^* \leqslant t_f$. The results of the least-square fits of Equation 2 to the experimental data are given in Table I, while reaction coefficients are plotted as a function of temperature in Fig. 2. In the temperature ranges from 800 to 1000 °C and from 700 to 1000 °C least-square fits gave the following reaction constants: in the first case $k = 10^{4.88 \pm 0.14} \exp[(-1.78 \pm 0.03)eV/kT]$ nm^2 s^{-1} (full line in Fig. 2) and in the second case $k = 10^{4.22 \pm 0.36} \exp[(-1.63 \pm 0.08)eV/kT]$ nm^2 s^{-1} (dashed line in Fig. 2). The decrease in activation energy with decreasing temperature indicates a change in the oxidation mechanism. This corresponds to the negative values of t_0 in Table I. Therefore we believe

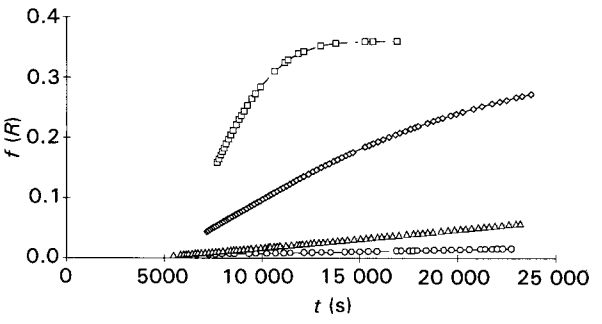

Figure 1 Oxidation of 20 nm SiC powders in air at the given temperatures; the function $f(R)$ is explained in the text. (○) 700 °C, (△) 800 °C, (◇) 900 °C, (□) 1000 °C.

TABLE I Parameters and results of a least-square fit of Equation 2 to the oxidation data of ultrafine SiC powders

Oxidation temperature (°C)	Fit interval (s)	Reaction constant ($nm^2\ s^{-1}$)	t_0 (s)	r^2 coefficient
400	3000–20 940	$1.46 \pm 0.07 \times 10^{-6}$	− 37 140	0.9196
500	4080–21 480	$4.48 \pm 0.12 \times 10^{-6}$	− 29 514	0.9715
600	4200–21 960	$2.02 \pm 0.060 \times 10^{-5}$	− 9120	0.9656
700	4860–22 240	$6.90 \pm 0.04 \times 10^{-5}$	− 2232	0.9978
800	5460–23 220	$3.21 \pm 0.006 \times 10^{-4}$	3726	0.9997
900	7140–23 700	$1.59 \pm 0.02 \times 10^{-3}$	3342	0.9845
1000	7680–9480	$6.66 \pm 0.08 \times 10^{-3}$	5064	0.9978

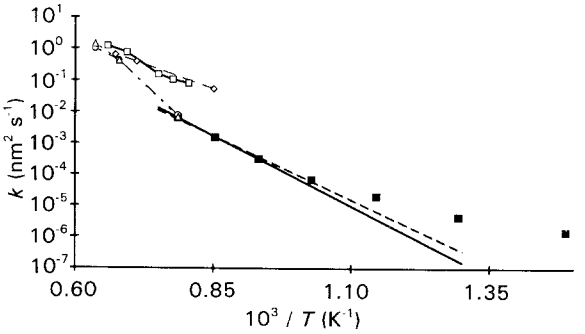

Figure 2 (■) Reaction constants of the oxidation of ultrafine SiC powders in air at different temperatures. The lines give the results of least-square fits using the values at (——) the three highest temperatures and (– – –) the four highest temperatures. Literature data are also included: (○, △) 40–63 μm SiC powder oxidized in air and in 1 bar O_2, respectively [11]; (◇) 40–63 μm SiC-powder oxidized in 1 bar O_2 [8]; (□) oxidation of a 6H α-SiC crystal (1 bar O_2) [12]. 1 bar oxygen data are multiplied by 0.201, see text.

that only at temperatures larger than 700 °C is diffusion-controlled oxidation the dominating mechanism.

Fig. 2 also shows the results of different oxidation measurements from other authors. To compare these oxidation measurements at 1 bar with the present investigation, a linear pressure dependence of the reaction constant was assumed ([10], see below). The slope of our data points (i.e. the activation energy) falls into the range of slopes of the literature data. The absolute values are relatively low compared to the given literature values. This might be a result of different powder morphologies and different particle size regimes (30 μm compared to 20 nm).

3.2. Logarithmic growth kinetics

As pointed out in the previous section, a parabolic oxidation law does not describe the oxidation of ultrafine particles at temperatures below 700 °C. We are therefore looking for a low-temperature oxidation mechanism which is able to describe our experimental data. In the case of silicon a logarithmic growth law for ultrafine oxide films was found at low temperatures [5]. These results can be explained by the Cabrera–Mott model. In this model the adsorbed oxygen produces electronic trap sites. These trap sites are populated by electrons from the metal or semiconductor and the corresponding contact potential difference V creates a field $E = V/x$ between metal and adsorbed oxygen (x = oxide layer thickness). As a result the barrier W to ion incorporation at the interface is reduced and the rate of oxide growth increases [13]:

$$\frac{dx}{dt} = N\Omega\nu \exp\left(\frac{-(W - qaE)}{kT}\right) \quad (6)$$

where N is the number of potentially mobile ions at the oxide interface. Ω the oxide volume per ion, ν the atomic vibration frequency, q the charge of the moving ion, a the half jump distance and kT has the usual meaning.

For small oxide thickness this equation was integrated by Ghez [14] giving

$$\frac{x_1}{x} = -\ln\left(\frac{t - t_0}{x^2}\right) - \ln(x_1 u)$$

with

$$x_1 = \left|\frac{qaV}{kT}\right| \qquad u = N\Omega\nu \exp\left(-\frac{W}{kT}\right)$$

$$t_0 = \text{constant} \quad (7)$$

In the case of silicon the transition from parabolic (or linear) growth to logarithmic growth is expected at about 500 °C. The actual value might be higher because Fehlner [5] found a logarithmic law even at 600 °C. This agreement with our experimental transition temperature made it evident that we should also apply a logarithmic growth law (Equation 7) to our data. Instead of the oxide layer thickness we use the fraction of completion R, which shows for small values of R a linear dependence on x:

$$R = 3x/zr \quad (8)$$

We can therefore rewrite Equation 7 to get

$$\frac{1}{R} = A\ln\left(\frac{t - t_0}{R^2}\right) + B$$

where

$$A = -\frac{zr}{3x_1}$$

$$B = -\frac{zr}{3x_1}\ln\left(\frac{9}{z^2r^2}x_1 u\right) = -\frac{zr}{3x_1}\left(\ln\frac{9x_1 N\Omega\nu}{z^2r^2} - \frac{W}{kT}\right) \quad (9)$$

In Fig. 3 the values of $1/R$ are plotted against $(t - t_0)/R^2$ and in Table II the results of least-square fits of Equation 9 to the data of Fig. 3 are given. The coefficients A and B, which are separately plotted in

TABLE II Parameters and results of a least-square fit of Equation 7 to the oxidation data of ultrafine SiC and Si–SiC powders

Type of powder	Oxidation temperature (°C)	Fit interval (s)	A	B (ln(s))	t_0 (s)	r^2 coefficient
SiC	23	$1.38–21.0 \times 10^6$	-5.785 ± 0.598	151.5 ± 12.8	1.26×10^6	0.921
SiC	400	3000–20 940	-1.446 ± 0.017	40.53 ± 0.25	2640	0.9949
SiC	500	4080–21 480	-1.563 ± 0.012	33.80 ± 0.17	2160	0.9978
SiC	600	4200–21 960	-2.311 ± 0.036	38.07 ± 0.48	3300	0.9916
SiC	700	4860–22 740	$-4.050 + 0.042$	55.22 ± 0.52	2880	0.9957
Si–SiC	400	2940–25 434	-1.210 ± 0.003	30.85 ± 0.05	2340	0.9997
Si–SiC	500	3608–25 536	-0.679 ± 0.001	17.58 ± 0.02	3000	0.999 85

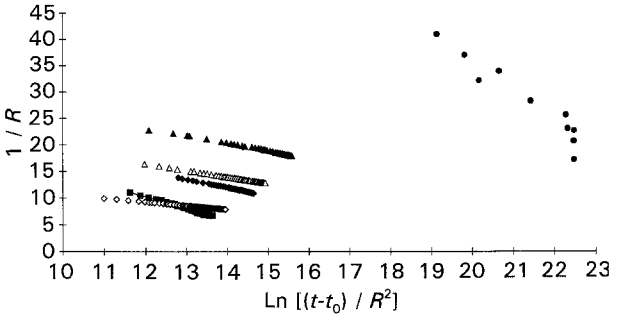

Figure 3 Low-temperature oxidation of SiC (closed symbols) and Si–SiC powders (open symbols). The data points are plotted according to Equation 9: (●) 23 °C; (▲, △) 400 °C; (◆, ◇) 500 °C; (■) 600 °C.

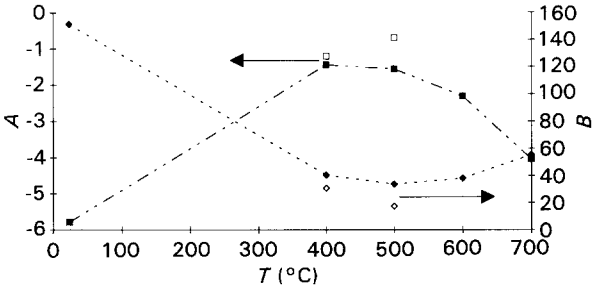

Figure 4 The coefficients A and B defined in the text plotted against the oxidation temperature (open symbols Si–SiC, closed symbols SiC powder).

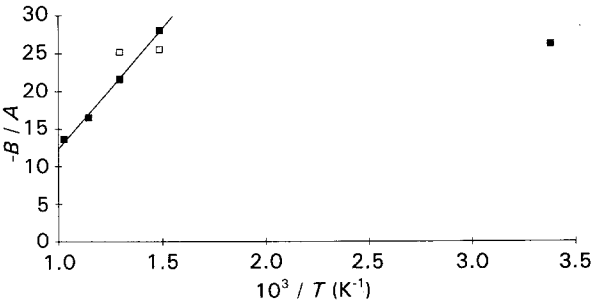

Figure 5 The quotient B/A defined in the text plotted against the inverse oxidation temperature: (□) Si–SiC, (■) SiC powder.

Fig. 4 against the oxidation temperature, do not reveal a distinct temperature dependence. The absolute values of the coefficients A and B are both smaller for Si–SiC than for SiC oxidation. This indicates a higher potential difference V across the oxide layer for the Si–SiC powders and therefore an enhanced incorporation of silicon ions into the oxide layer.

The quotient B/A (Fig. 5) is, in the temperature range between 400 and 700 °C, proportional to $1/T$ as expected from Equation 9. A least-square fit to the SiC and Si–SiC data points (straight line in Fig. 5) gives an activation energy of 2.75 ± 0.12 eV. This value is larger than the values found in silicon (1.4–1.9 eV [15]). A possible reason is that the Si–C bond energy is higher than the Si–Si bond energy. Using $\Omega = 0.045\ \text{nm}^3$, $\nu = 10^{12}\ \text{s}^{-1}$ and $x_1 \approx 15$ nm ($A \simeq -2$) we also calculated the surface concentration N as $3 \times 10^{16}\ \text{m}^{-2}$. At room temperature the value of B/A is lower by a factor of three than expected from the high-temperature data (Fig. 5). Similar results are stated by Fehlner [5] for the oxidation of silicon. He drew the conclusion that the activation energy W and also the voltage V across the oxide is temperature-dependent.

In order to calculate the oxidation of SiC powders for intermediate temperatures as well, we assumed a linear behaviour of the coefficients A and B as drawn in Fig. 4.

3.3. First-order kinetics

The rate of formation of the first oxide layer on silicon carbide powders should be proportional to the oxide free surface and we therefore expect first-order kinetics, which we evaluate in terms of mass changes:

$$\frac{\mathrm{d}}{\mathrm{d}t}\left(\frac{\Delta m}{m_0}\right) = -\alpha\left(\frac{\Delta m}{m_0} - \frac{m_{\text{final}}}{m_0}\right) \rightarrow \frac{\Delta m}{m_0}$$

$$= \frac{m_{\text{final}}}{m_0}[1 - \exp(-\alpha t)] \qquad (10)$$

where $\Delta m/m_0$ is the relative mass change, m_{final}/m_0 the final mass change and α the reaction constant.

The total mass change $\Delta m/m_0$ during our room-temperature oxidation experiment was 0.276%, which is smaller by a factor of 3.96 than expected from the chemical analysis of the oxidized powder (O content: 1.75 wt %). We therefore conclude that after the HF treatment the samples still contain a certain amount of oxygen (corresponding to a mass change $\Delta m_0/m_0$). We can now rewrite Equation 10 as

$$\frac{\Delta m_0 + \delta m}{m_0} = \frac{m_{\text{final}}}{m_0}\{1 - \exp[-\alpha(t + t_0)]\} \rightarrow$$

$$\ln\left(1 - \frac{\delta m}{\delta m_g}\right) = -\alpha(t + t_0) - \ln\left(\frac{\delta m_g}{m_{\text{final}}}\right)$$

$$= -\alpha(t + t_0) + 1.38 \qquad (11)$$

TABLE III Results of least-square fits to the room-temperature oxidation of ultrafine SiC powder

Fit	Time interval (s)	α (s^{-1})	t_0 using fit and Equation 11	t_0 using α and Equation 12	r^2 coefficient
A	1680–9420	$1.25 \pm 0.03 \times 10^{-4}$	10396	11040	0.9858
B	1680–27960	$7.97 \pm 0.13 \times 10^{-5}$	18731	17315	0.9824

where δm (δm_g) is the (total) mass change during our oxidation experiment and t_0 is the oxidation time corresponding to the mass change given by

$$\Delta m_0/m_{final} = 1 - 3.96^{-1} = 0.748 = 1 - \exp(-\alpha t_0)$$

$$\text{i.e } t_0 = 1.38/\alpha \qquad (12)$$

The results of our oxidation experiments are plotted according to Equation 11 in Fig. 6. The linear behaviour confirms our hypothesis that the oxidation for low degrees of completion R follows first-order kinetics. For longer times we observe deviations from the linear behaviour. They are due to the logarithmic scale and uncertainties in the final degree of oxidation. Therefore we performed least-square fits only for times less than 30000 s. The results for two different intervals are given in Table III. The time constant α of fit A is in good agreement with the result found in a similar experiment using SiC powder with a particle size of 0.1 μm ($\alpha = 1.56 \times 10^{-4}\ s^{-1}$ [16]). Also the final degree of oxidation (1.75 wt% O corresponds to $3.52 \times 10^{-7}\ kg\,m^{-2}$) is comparable to their result ($2.24 \times 10^{-7}\ kg\,m^{-2}$).

It should be mentioned that our degree of oxidation corresponds to an oxide layer thickness of 0.16 nm. This is about half the thickness of a monolayer of SiO_2 (0.36 nm), which might indicate that only half of the silicon bonds are occupied by oxygen atoms.

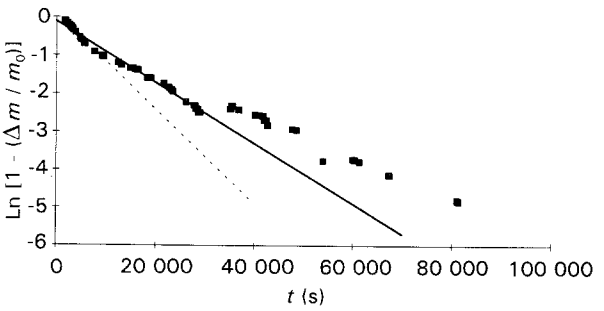

Figure 6 (■) Plot of the room-temperature oxidation data of ultrafine SiC powders according to Equation 11. The straight lines show the results of least-square fits for different time intervals: (– – –) 0–10000 s, (——) 0–30000 s.

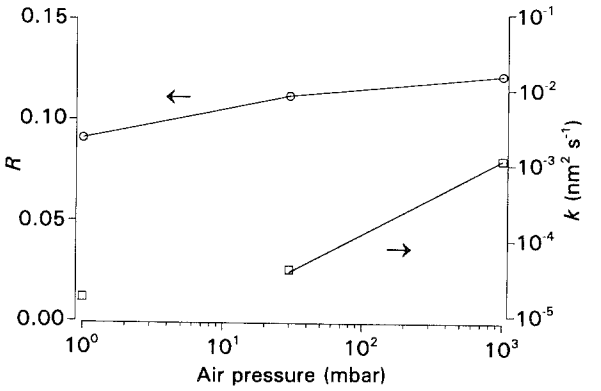

Figure 7 (□) Reaction constants of ultrafine Si–SiC powders oxidized at 800 °C in air at the given pressures; (○) fractions of completion R after 10^5 s for the oxidation in air at 500 °C.

3.4. Pressure dependence

The reaction constant of ultrafine Si–SiC powders oxidized in a pressure of 1 mbar, 30 mbar and 1 bar air at 800 °C is given in Fig. 7. Between 30 mbar and 1 bar the pressure dependence is close to a linear one. This corresponds to results given in the literature [3, 11, 13] and it implies that at 800 °C the rate-determining step during the oxidation of SiC is the diffusion of O_2 through the vitreous SiO_2 layer [17].

At lower pressures the reaction constant is much higher than expected from a linear pressure dependence. As described below, the logarithmic growth kinetics shows only a minor pressure dependence. As a result the oxidation due to this process will dominate even at higher temperatures if the oxygen pressure is reduced. Therefore a deviation from the linear pressure dependence is found at 800 °C and 1 mbar oxygen pressure. Also the observed decrease of the r^2 coefficient from 0.999 to 0.949 with decreasing oxygen pressure (1000 to 1 mbar) suggests a change in the oxidation mechanism.

The pressure dependence of the oxidation of ultrafine Si–SiC powders at 500 °C is also shown in Fig. 7. Instead of plotting the constants A and B of Equation 9 the fraction of completion R after 10^4 s at 500 °C is given. The fraction of completion is chosen here because it is a direct measure of the degree of oxidation. The results show that even a reduction of the oxygen pressure by a factor of 1000 only slightly (26%) reduces the amount of oxidation. This is due to the logarithmic growth kinetics. Oxidation will only be effected by the oxygen pressure if insufficient oxygen molecules are available at the SiO_2 surface. If the observed minor pressure dependence also holds at room temperature, ultrafine SiC powders should be stored only under extremely low partial oxygen pressures ($\ll 0.2$ mbar, corresponding to 1 mbar air) and only for a limited time.

3.5. Oxidation maps

We tried to sum up our results on the oxidation of ultrafine SiC powders in air in Fig. 8. In this figure the time which passes until a certain degree of completion

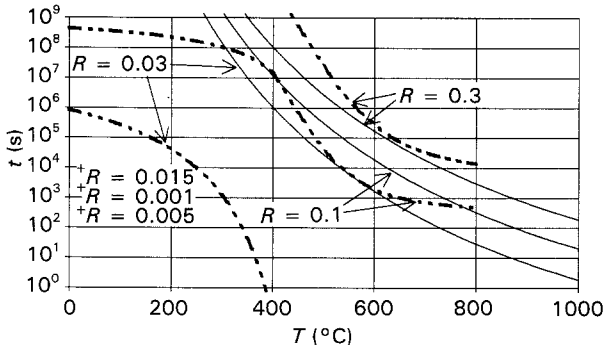

Figure 8 "Oxidation map" of ultrafine SiC powders: the time which passes until the given degree of oxidation completion R is reached is plotted against the oxidation temperature (oxidation in air): (——) diffusion control, (– – –) Cabrera–Mott-like behaviour, (+) results due to first-order kinetics (only at room temperature).

R is reached is plotted against the oxidation temperature. It is found that after the formation of the first oxide monolayer a Cabrera–Mott-like mechanism (B) operates for small values of R by orders of magnitude faster than diffusion-controlled oxidation (A).

Due to the minor pressure dependence of the Cabrera–Mott-like mechanism (B), storing of ultrafine (Si–)SiC powders without oxidation is only possible under extremely low O_2 pressures ($\ll 0.2$ mbar). If storage is restricted to a few weeks ($\sim 10^6$ s), oxygen contents below 2.5 wt % ($R < 0.03$) are expected (Fig. 8).

4. Conclusions

The oxidation of ultrafine SiC powders in the temperature regime below 1000 °C can be described by three different mechanisms. Starting with the highest investigated temperatures we found a "normal" diffusion-controlled oxidation mechanism in the temperature range between 700 and 1000 °C. An Arrhenius plot of the reaction constant led to activation energies of about 1.6–1.8 eV, which is in good agreement with oxidation data of conventional powders.

At temperatures below 700 °C the dominating oxidation mechanisms can be described by a Cabrera–Mott-like equation. The resultant constants are physically meaningful and similarities to the low-temperature oxidation of silicon are obvious. An energy barrier for ion incorporation into the oxide was determined to be about 2.8 eV.

At low degrees of completion ($R < 0.0223$) the oxidation follows first-order kinetics with a reaction constant of $1.25 \times 10^{-4}\ s^{-1}$. After the formation of a half monolayer of SiO_2 this reaction is completed.

As a more general conclusion, the present investigation showed that ultrafine SiC powders are extremely sensitive to oxidation. Storage of such powders for a long period of time even at room temperature leads, at least in air, to considerable oxidation.

Acknowledgements

The authors would like to thank Mr Rauwald (Institut für Angewandte Werkstofforschung, KFA Jülich, Germany) for performing the thermobalance measurements. They are also indebted to J. Förster (Institut für Laser- und Plasmaphysik, Universität, Düsseldorf, Germany) for producing the ultrafine powders and to Dr Heckner (Institut für Chemische Analysen, KFA Jülich, Germany), who performed the chemical analyses of the powders.

References

1. S. C. SINGHAL, in "Ceramics for High-Performance Applications", Proceedings of 2nd Army Materials Technology Conference, Hyannis, Massachusetts, November 1973, edited by J. J. Burke, A. E. Gorom, R. N. Katz (Metals and Ceramics Information Center) p. 533.
2. S. DUTTA, *J. Mater. Sci.* **19** (1984) 1307.
3. K. L. LUTHRA, *J. Amer. Ceram. Soc.* **74** (1991) 1095.
4. Gmelin Handbook, Silicon, Part B, Section 3, p. 327.
5. F. P. FEHLNER, *J. Electrochem. Soc.: Solid-State Sci. Technol.* **119** (1972) 1723.
6. G. J. DECLERCK, in Proceedings of NATO Advanced Study Institute on Microelectronic Materials and Processes, Ciocco, Italy, June 1986, edited by R. A. Levy (Klower Academic) p. 79.
7. J. FÖRSTER, M. von HOESSLIN, J. H. SCHÄFER, J. UHLENBUSCH and W. VIÖL, in Proceedings of 10th International Symposium on Plasma Chemistry, FRG, 1991, Vol. 1, p. 1.
8. P. J. JORGENSEN, M. E. WADSWORTH and I. B. CUTLER, *J. Amer. Ceram. Soc.* **42** (1959) 613.
9. R. E. CARTER, *J. Chem. Phys.* **34** (1961) 2010.
10. K. MOTZFELD, *Acta Chem. Scand.* **18** (1964) 1596.
11. R. EBI, thesis, University of Karlsruhe, Germany (1973).
12. R. C. HARRIS and R. L. CALL, in "Silicon Carbide", edited by R. C. Marshall, J. W. Forest and C. E. Ryan (University of South Carolina Press, Coloumbia, 1973) p. 329.
13. F. P. FEHLNER, "Low-Temperature Oxidation" (Wiley, New York, 1986) p. 18.
14. R. GHEZ, *J. Chem. Phys.* **58** (1973) 1838.
15. F. P. FEHLNER, "Low-Temperature Oxidation" (Wiley, New York, 1986) p. 180.
16. R. LENK, A. F. KRIWOSTSCHEPOW and J. G. FROLOW, *Chem. Chem. Technol.* (in Russian) **54**(148) (1987) 48.
17. F. P. FEHLNER, "Low-Temperature Oxidation" (Wiley, New York, 1986) p. 223.

Received 18 March 1993
and accepted 16 February 1994